Coen et al., http://www.jcb.org/cgi/content/full/jcb.201201076/DC1

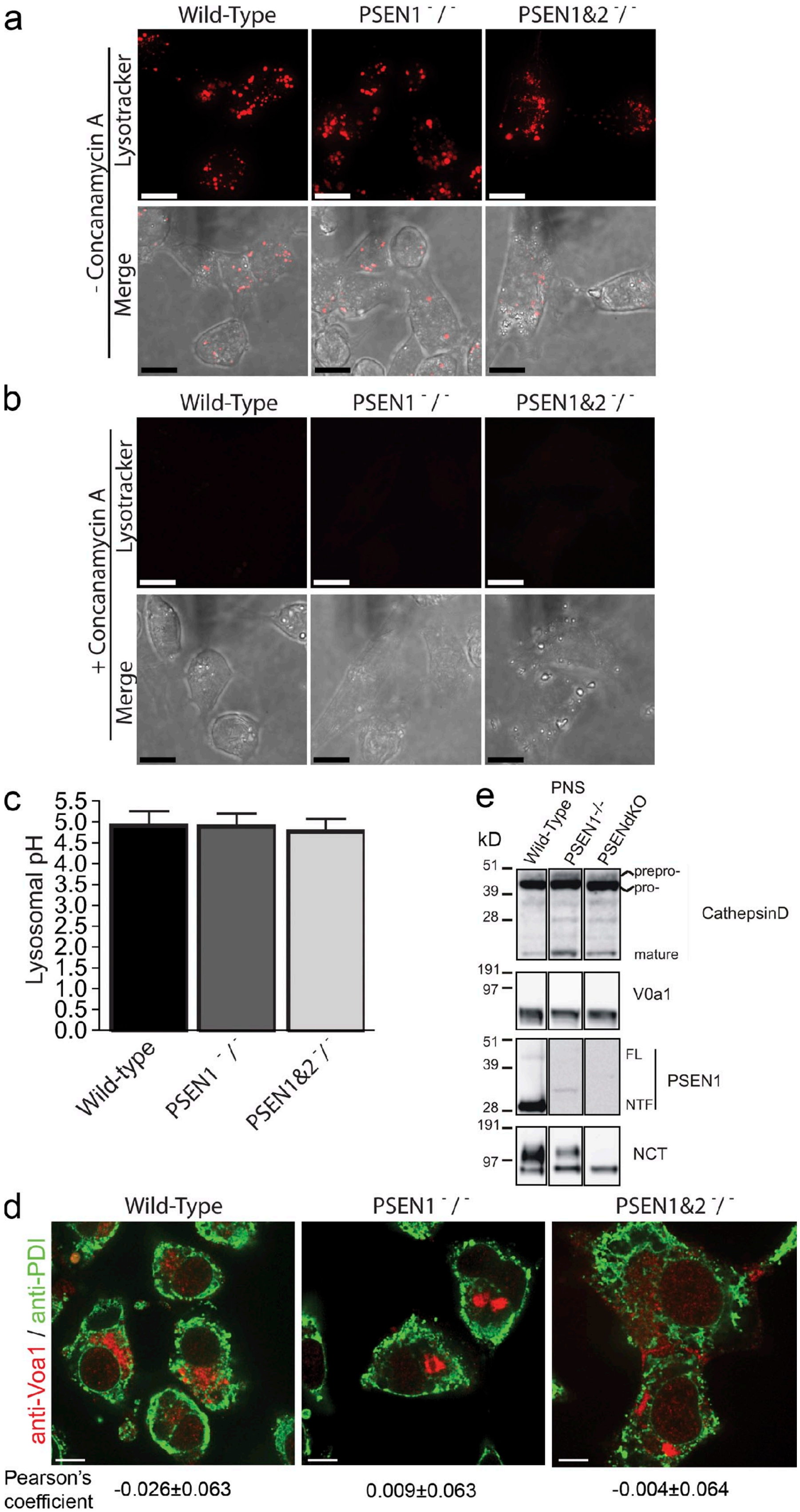

Figure S1. **Characterization of V-ATPase function in blastocyst-derived extraembryonic endoderm cells that lack PSENs.** (a and b) Blastocysts derived from WT, PSEN1 $^{-/-}$, and PSENdKO mice were analyzed by LysoTracker staining with (b) and without (a) concanamycin A treatment. The top panels represent z projections of the LysoTracker fluorescence, whereas the bottom panels depict merged z projections of cells imaged for LysoTracker fluorescence and by brightfield. Bars, 18 µm. (c) The bar graph represents the measured lysosomal pH for WT, PSEN1 $^{-/-}$, and PSENdKO blastocysts (error bars indicate means ± SEM; *n* = 2–3, 30–40 cells). (d) The cellular distribution of the V0a1 subunit of the V-ATPase and the resident ER protein, PDI, were analyzed by immunofluorescence. Shown are representative xy confocal images for WT, PSEN1$^{-/-}$, and PSEN1&2$^{-/-}$ blastocysts with V0a1 antibody staining in red and PDI antibody staining in green. The mean Pearson's coefficient ± SD for colocalization of V0a1 with PDI is displayed below each image. Bars, 10.1 µm. (e) Western blot analysis of PNS derived from WT, PSEN1$^{-/-}$, and PSENdKO blastocysts for endogenous cathepsin D. Immunoreactive bands representing prepro- and pro-cathepsin, and in particular mature processed cathepsin D, are reminiscent in all three cell lines, which indicates normal maturation and levels of cathepsin D in WT and PSEN-deficient blastocysts. Expression levels of V0a1 were also not affected by PSEN deficiency. NCT is used as a control to indicate decreased levels of mature NCT in PSEN1$^{-/-}$ and only immature NCT in PSENdKO blastocysts.

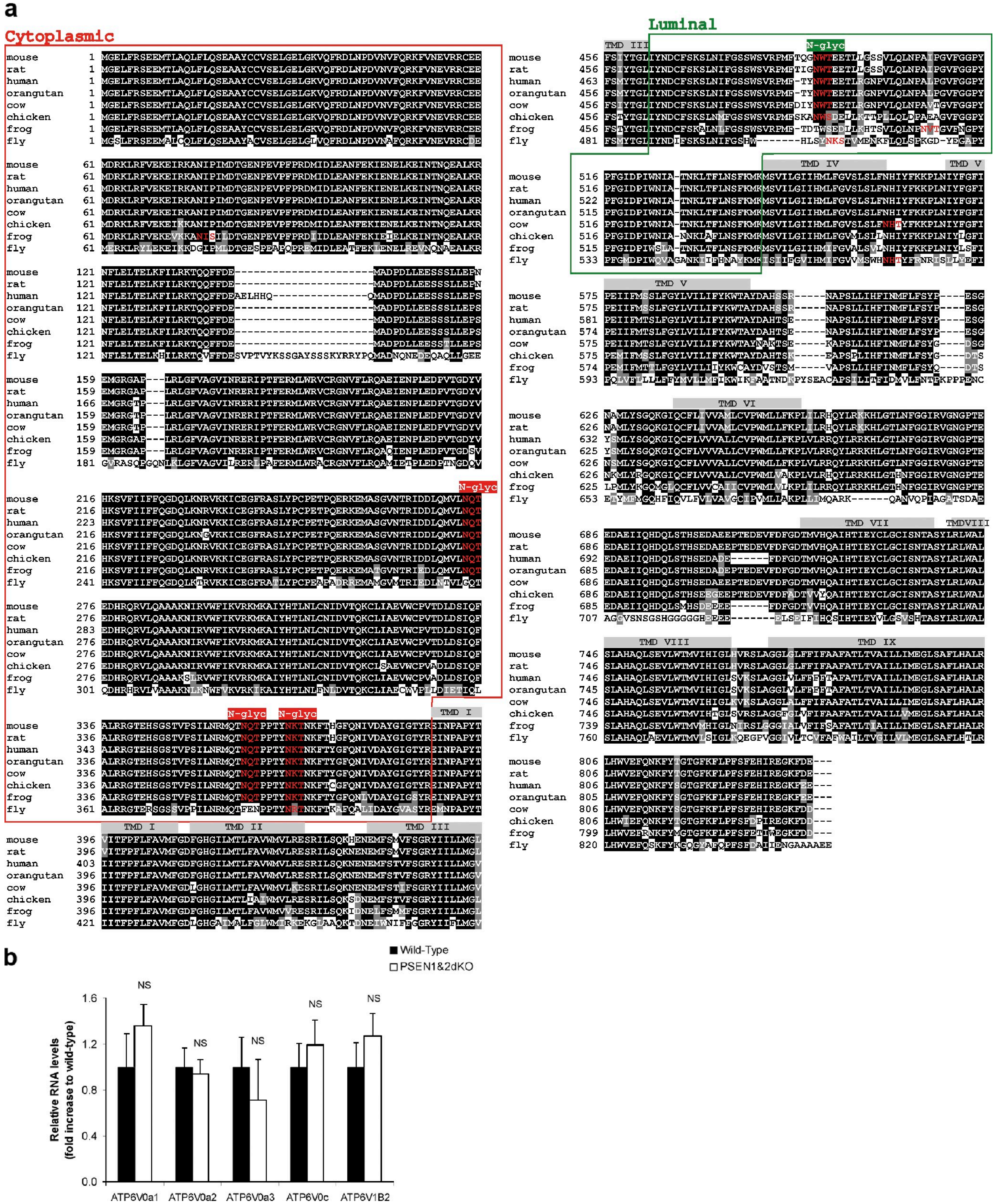

Figure S2. **Sequence alignment and expression levels of V0a1 subunit orthologues.** (a) Sequence alignment of V0a1 subunit orthologues predicts one conserved N-glycosylation site. Four potential N-glycosylation sites were present in the V-ATPase subunit V0a1, of which only one (N_{489}WTE) was available in the ER lumen. Multiple sequence alignment of the V0a1 subunit (http://www.ebi.ac.uk/Tools/msa/clustalw2/) of mouse (NCBI Protein database accession no. NP_058616.1), rat (NP_113792.2), human (NP_001123492.1), orangutan (NP_001126661.1), cow (NP_777179.1), chicken (NP_990055.1), frog (NP_001080294.1), and fly (NP_001163768.1) shows high conservation over the shown species (black). Transmembrane domains (TMD) are indicated with gray bars (Nishi and Forgac, 2000). N-glycosylation motifs were predicted using the NetNGlyc 1.0 software (http://www.cbs.dtu.dk/services/NetNGlyc/). According to the current topology model for the V-ATPase, nonfunctional N-glycosylation sites present in the N-terminal cytoplasmic domain are depicted with red bars, whereas the N-glycosylation motif between TMD III and IV, present in the luminal part of the V0a1 subunit, is depicted in green. Note that Asn-Xaa-Ser/Thr motifs are highlighted in red. (b) RNA levels of V0a subunits are not significantly altered between PSEN-deficient and WT MEFs. RNA levels for V0a1, V0a2, and V0a3 were measured by RT-qPCR and quantified according the comparative ΔΔCt method in MEF WT versus PSENdKO. V0c and V1B2 were used as a control (error bars indicate mean ± SEM; *n* = 2–5; NS, one-way ANOVA).

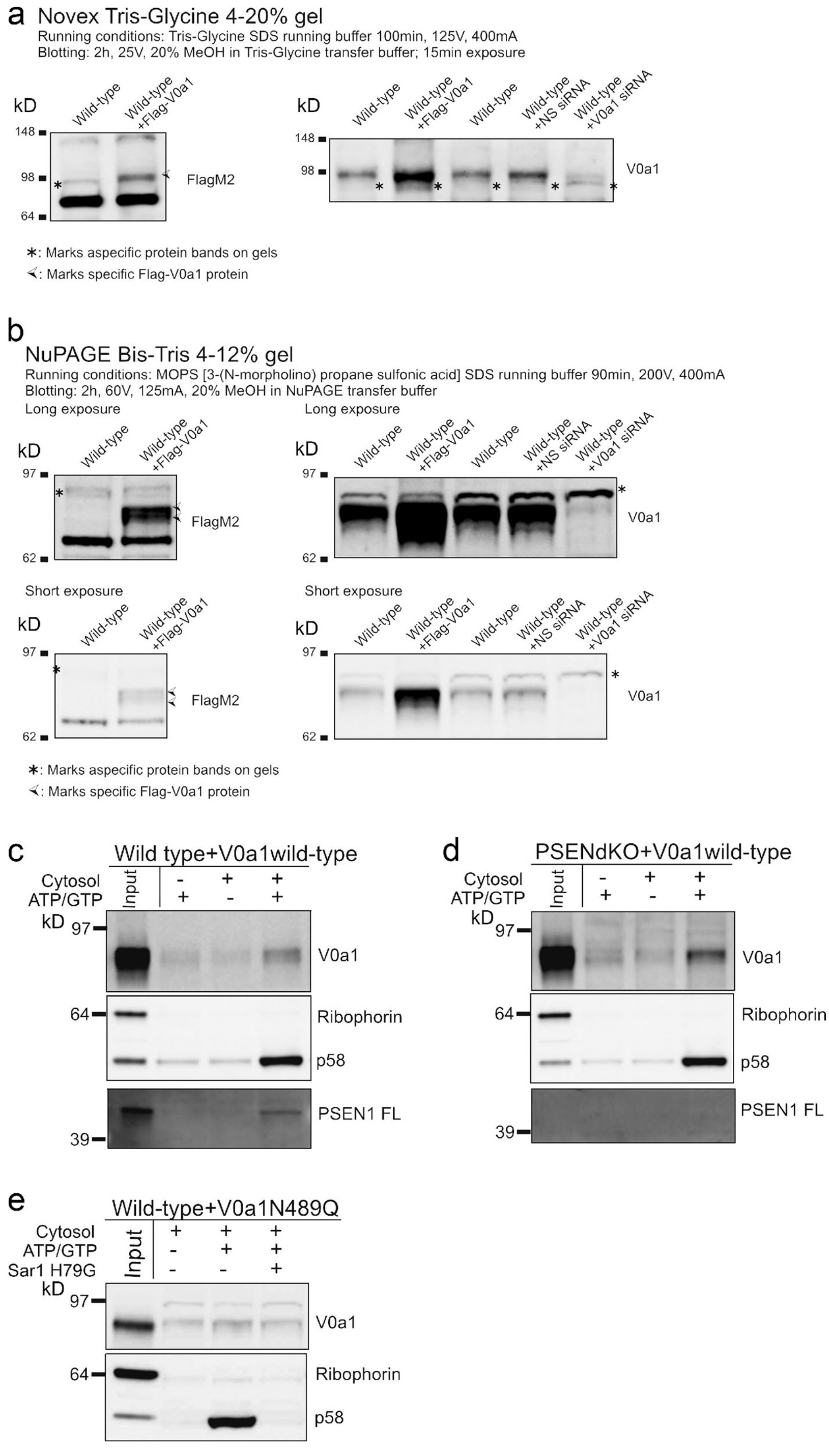

Figure S3. **Characterization of V0a1 subunit in total cell extracts and in vitro ER exit assays.** (a and b) Western blot analysis of V-ATPase subunit V0a1 on different gel types and running buffers. (a) A Novex Tris-Glycine 4–20% gel run in Tris-Glycine SDS running buffer (conditions used as in Lee et al., 2010) and (b) a NuPAGE Bis-Tris 4–12% gel run in MOPS SDS running buffer were used for the Western blotting of total cell lysates from WT MEFs (either non-transfected, overexpressing V0a1, or siRNA down-regulated). Cells were seeded for 24 h (overexpression) or 48 h (down-regulation) before total lysates were prepared. (c–e) The V0a1 subunit is actively transported out of the ER in WT and PSENdKO cells. Western blot analysis of in vitro ER-budding assays performed in permeabilized (c) WT and (d) PSENdKO MEFs, with the input (first lane) and budding reactions (lanes 2–4). No COPII budding vesicles were recovered when cytosol was omitted (lane 2), or in the absence of an ATP/GTP regenerating system (lane 3). Full budding was reconstituted in the presence of cytosol and ATP/GTP (lane4), as indicated by the release of p58/ERGIC-53 in the vesicle fraction. ER budding is selective, as Ribophorin I, a component of the OST complex and resident protein in the ER, was not sorted into COPII vesicles. Exogenously expressed V0a1 subunit readily exits the ER in both WT (c) and PSENdKO MEF (d). For WT cells, ER exit of full-length PSEN1 is shown as an additional positive control. (e) An in vitro ER-budding assay demonstrating that the exogenously expressed glycosylation-deficient V0a1 $N_{489}Q$ mutant also exits the ER. Release in de novo COPII-coated vesicles was inhibited by the addition of $Sar1^{H79G}$, a dominant-active Sar1 GTPase that selectively blocks ER budding, as also observed for p58/ERGIC-53.

Table S1. **Specific siRNA oligos against mouse ATP6 V0a1**

Oligo	Sequence
V0a1 oligos	
	5′-UGAUUAACCGGGAGCGGAU-3′
	5′-AGACAUCUUAUCCGGAAUA-3′
	5′-CGAGAUGGGAAGAGGCGCA-3′
	5′-GCUAAGAACAUCCGCGUCU-3′
Non-specific siRNA oligo	
	5′-CGUACGCGGAAUACUUCGAdTdT-3′

Table S2. **Primers for qPCR**

Gene isoform	Sense/antisense	Primers	Nucleotides	Accession no.
HPRT-1	Forward	5′-GCTTTCCCTGGTTAAGCAGTACA-3′	23	NM_013556.2
	Reverse	5′-GAGAGGTCCTTTTCACCAGCAA-3′	22	
GUSB	Forward	5′-TCGCCGACTTCATGACGAA-3′	19	NM_010368.1
	Reverse	5′-GCTGTCTCTGGCGAGTGAAGA-3′	21	
ATP6 V0a1	Forward	5′-GAAATGGCTTCCGGAGTCAA-3′	20	NM_001243050.1
	Reverse	5′-TGGTCCTCCGTCTGATTCAGA-3′	21	
ATP6 V0a2	Forward	5′-AGCAAGACACACGGGCTCTAC-3′	21	NM_011596.4
	Reverse	5′-ACCGTGAGAGCCACCAACAC-3′	20	
ATP6 V0a3	Forward	5′-GGGAGCTGCTGGGCTAGAAGCAA-3′	23	NM_016921.3
	Reverse	5′-GCCGGACGTCTACCACGAAGC-3′	21	
ATP6 V0a4	Forward	5′-GTCCAGCCCATTGCAGGCATTC-3′	22	NM_080467.3
	Reverse	5′-AGCAATACGCAGCCTCCACCTG-3′	22	
ATP6 V0c	Forward	5′-GTCCGCCATGGTCTTCAG-3′	18	NM_009729.3
	Reverse	5′-CAGCTCTGGCCTCATGACT-3′	19	
ATP6 V1B2	Forward	5′-CAATGTCTGCCTTTTTTTGAATCTG-3′	25	NM_007509.3
	Reverse	5′-GCCAGGCGAGGAGTGATG-3′	18	

References

Lee, J.H., W.H. Yu, A. Kumar, S. Lee, P.S. Mohan, C.M. Peterhoff, D.M. Wolfe, M. Martinez-Vicente, A.C. Massey, G. Sovak, et al. 2010. Lysosomal proteolysis and autophagy require presenilin 1 and are disrupted by Alzheimer-related PS1 mutations. *Cell*. 141:1146–1158. http://dx.doi.org/10.1016/j.cell.2010.05.008

Nishi, T., and M. Forgac. 2000. Molecular cloning and expression of three isoforms of the 100-kDa a subunit of the mouse vacuolar proton-translocating ATPase. *J. Biol. Chem.* 275:6824–6830. http://dx.doi.org/10.1074/jbc.275.10.6824